Inorg. Chem. **2004**, *43*, 945–953

Monomeric, Tetrameric, and Polymeric Copper Di-*tert*-butyl Phosphate Complexes Containing Pyridine Ancillary Ligands†,⊥

Ramaswamy Murugavel,*,‡ Malaichamy Sathiyendiran,‡ Ramasamy Pothiraja,‡ Mrinalini G. Walawalkar,§ Talal Mallah,*,|| and Eric Riviére||

Department of Chemistry, Indian Institute of Technology—Bombay, Powai, Mumbai-400 076, India, Applied Chemistry Division, Mumbai University Institute of Chemical Technology (UICT), Matunga, Mumbai-400 019, India, and University Paris-Sud, Bat. 420, Laboratoire de Chimie Inorganique, UMR CNRS 8613, 91405 Orsay-France, France

Received August 8, 2003

The reaction of di-*tert*-butyl phosphate ((^{t}BuO)$_2$P(O)(OH), dtbp-H) with copper acetate in the presence of pyridine (py) and 2,4,6-trimethylpyridine (collidine) has been investigated. Copper acetate reacts with dtbp-H in a reaction medium containing pyridine, DMSO, THF, and CH_3OH to yield a one-dimensional polymeric complex $[Cu(dtbp)_2(py)_2(\mu\text{-}OH_2)]_n$ (**1**) as blue hollow crystalline tubes. The copper atoms in **1** are octahedral and are surrounded by two terminal phosphate ligands, two pyridine molecules, and two bridging water molecules. The μ-OH_2 ligands that are present along the elongated Jahn–Teller axis are responsible for the formation of the one-dimensional polymeric structure. Recrystallization of **1** in a DMSO/THF/CH_3OH mixture results in the reorganization of the polymer and its conversion to a more stable tetranuclear copper cluster $[Cu_4(\mu_3\text{-}OH)_2(dtbp)_6(py)_2]$ (**2**) in about 60% yield. The molecular structure of **2** is made up of a tetranuclear core $[Cu_4(\mu_3\text{-}OH)_2]$ which is surrounded by six bidentate bridging dtbp ligands. While two of the copper atoms are pentacoordinate with a tbp geometry, the other two copper atoms exhibit a pseudooctahedral geometry with five normal Cu–O bonds and an elongated Cu–O linkage. The pentacoordinate copper centers bear an axial pyridine ligand. The short Cu···Cu nonbonded distances in the tetranuclear core of **2** lead to magnetic ordering at low temperature with an antiferromagnetic coupling at ~20 K ($J_P = -44$ cm^{-1}, $J_c = -66$ cm^{-1}, $g = 2.25$, and $\rho = 0.8\%$). When the reaction between di-*tert*-butyl phosphate (dtbp-H) and copper acetate was carried out in the presence of collidine, large dark-blue crystals of monomeric copper complex $[Cu(dtbp)_2(collidine)_2]$ (**3**) formed as the only product. A single-crystal X-ray diffraction study of **3** reveals a slightly distorted square-planar geometry around the copper atom. Thermogravimetric analysis of **1**–**3** revealed a facile decomposition of the coordinated ligands and dtbp to produce a copper phosphate material around 500 °C. An independent solid-state thermolysis of all the three complexes in bulk at 500–510 °C for 2 days produced copper pyrophosphate $Cu_2P_2O_7$ along with small quantities of $Cu(PO_3)_2$ as revealed by DR–UV spectroscopic and PXRD studies.

Introduction

The reaction between a transition metal ion and a phosphorus acid or ester has attracted the attention of inorganic, bioinorganic, biological, and materials chemists in view of its relevance in metal-catalyzed phosphate ester hydrolysis,[1−3] synthesis of cagelike and extended framework phosphates,[4−6] and generation of single molecular magnets.[7]

* To whom correspondence should be addressed. E-mail: rmv@iitb.ac.in (R.M.). Fax: +91 (22) 2572 3480 (R.M.).

† Molecular Metal Phosphates. 5. Part 4: Murugavel, R.; Sathiyendiran, M.; Pothiraja, R.; Butcher, R. J. *Chem. Commun.* **2003**, 2546. Parts 1−3: see ref 17−19.

‡ Indian Institute of Technology.
§ Mumbai University Institute of Chemical Technology (UICT).
|| University Paris-Sud (magnetic studies).

⊥ This work is dedicated to Professor P. T. Manoharan.

(1) Chin, J. *Acc. Chem. Res.* **1991**, *24*, 145.
(2) Williams, N. H.; Takasaki, B.; Wall, M.; Chin, J. *Acc. Chem. Res.* **1999**, *32*, 485.
(3) Jurek, P. E.; Martell, A. E. *Inorg. Chem.* **1999**, *38*, 6003.
(4) Walawalkar, M. G.; Roesky, H. W.; Murugavel, R. *Acc. Chem. Res.* **1999**, *32*, 117.
(5) (a) Neeraj, S.; Forster, P. M.; Rao, C. N. R.; Cheetham, A. K. *Chem. Commun.* **2001**, 2716. (b) Dan, M.; Udayakumar, D.; Rao, C. N. R. *Chem. Commun.* **2003**, 2212.
(6) Lugmair, C. G.; Tilley, T. D.; Rheingold, A. L. *Chem. Mater.* **1999**, *11*, 1615.

10.1021/ic0349508 CCC: $27.50
Published on Web 12/30/2003

An interesting and common element in all metal phosphates is the presence of a number of hydrogen bonds, which often richly contributes to the understanding of the associated chemistry. In particular, H-bonding found in metal phosphates has been recently implicated to shed light on the mechanism of metal-assisted phosphate ester hydrolysis.[8,9] The well-demonstrated ability of phosphate ligands with bulky alkyl or aryl substituents acting as monodentate ligands, leaving the phosphoryl P═O group free, results in the formation of interesting intra- and intermolecular hydrogen-bonding networks in the solid state and in solution.[9]

We have been interested for sometime in employing silanols ($R_nSi(OH)_{4-n}$) and phosphorus acids ($RP(O)(OH)_2$, $R_2P(O)(OH)$, etc.) as ligands in nonmetal and metal chemistry with the objective of forming suitable model compounds for metallosilicates and phosphate materials.[9−20] There has been an outburst of activity in metal molecular metal phosphate/phosphonate chemistry due to the use of these molecular compounds in materials science related applications.[17−28] In particular, our own interest in the chemistry of di-*tert*-butyl phosphate [(^{t}BuO)$_2$P(O)(OH)] is due to the ability of this ligand to bind a variety of metal ions and also the high solubility of the resultant complexes in a variety of organic solvents owing to the presence of bulky *tert*-butoxide groups on the surface of the inorganic structures.[17−19] Moreover, owing to the very low thermal stability of the P−OBu^t group of dtbp (which results in a facile β-hydride elimination and the formation of P−OH group with concomitant evolution of isobutene gas), the transition metal−dtbp complexes have proven to be excellent precursors for the preparation of metal phosphate materials via solid-state thermolysis conditions at fairly low temperatures (Scheme 1).[17−19] While Tilley et al. have reported on the use of aluminum, titanium, and zinc dtbp complexes as precursors for the preparation of respective metal phosphate materials,[28] our recent work in this area has demonstrated the use of polymeric complexes of the formula [M(dtbp)$_2$] (M = Mn, Co, Cu, Cd) as ideal precursors for the preparation of high-purity metaphosphate materials.[17−19]

Scheme 1. Preparation of Phosphate Materials from Molecular Complexes

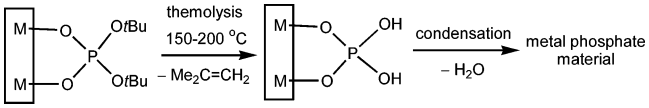

Scheme 2. Synthesis of [Cu(dtbp)$_2$] and Its Conversion to [Cu(PO$_3$)$_2$][17]

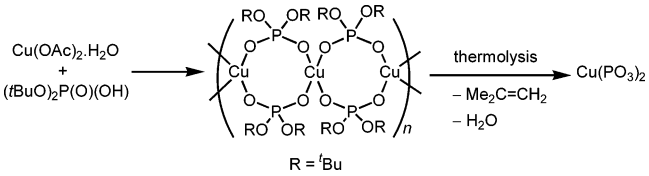

Continuing our interest on metal−dtbp complexes, we have now studied the reaction of copper acetate with dtbp-H in the presence of donor solvents and isolated three novel copper−dtbp complexes, which exist in monomeric, tetrameric, and polymeric forms, respectively. The results of this investigation, describing the synthesis, spectral studies, single-crystal X-ray structures, solid-state thermolysis studies, and low-temperature magnetic studies, are reported in this contribution. The formation of interesting hydrogen bonds in these molecules due to the presence of uncoordinated phosphoryl P═O groups is also highlighted in this paper.

Results and Discussion

Synthesis and Spectra. The reaction between copper acetate and dtbp-H, investigated by us recently under a variety of conditions, led to the formation of [Cu(dtbp)$_2$]$_n$, in which the dtbp anion behaves as a bridging bidentate ligand to result in the formation of an extended one-dimensional polymeric chain (Scheme 2).[17] This polymer was found to be thermally very labile and produced high-purity Cu(PO$_3$)$_2$ material under solid-state thermolysis conditions. In the present study, we chose to investigate this reaction further in detail and examine the products obtained when additional donor solvents or ligands are used.

The reaction of Cu(OAc)$_2$·H$_2$O with 2 equiv of dtbp-H in the presence of pyridine and pyrazine bases in a solvent mixture containing CH$_3$OH, THF, and DMSO initially yielded a blue solution from which a dark-blue crystalline **1** was obtained. Examination of **1** under microscope revealed

(7) Brechin, E. K.; Coxall, R. A.; Parkin, A.; Parsons, S.; Tasker, P. A.; Winpenny, R. E. P. *Angew. Chem., Int. Ed.* **2001**, *40*, 2700.
(8) Chin, J.; Chung, S.; Kim, D. H. *J. Am. Chem. Soc.* **2002**, *124*, 10948.
(9) (a) Murugavel, R.; Sathiyendiran, M.; Pothiraja, R.; Butcher, R. J. *Chem. Commun.* **2003**, 2546. (b) Sathiyendiran, M. Ph.D. Thesis, IIT-Bombay, 2003.
(10) Murugavel, R.; Chandrasekhar, V.; Roesky, H. W. *Acc. Chem. Res.* **1996**, *29*, 183.
(11) Murugavel, R.; Voigt, A.; Walawalkar, M. G.; Roesky, H. W. *Chem. Rev.* **1996**, *96*, 2205.
(12) Murugavel, R.; Prabusankar, G.; Walawalkar, M. G. *Inorg. Chem.* **2001**, *40*, 1084.
(13) Murugavel, R.; Walawalkar, M. G.; Prabusankar, G.; Davis, P. *Organometallics* **2001**, *20*, 2639.
(14) Murugavel, R.; Shete, V. S.; Baheti, K.; Davis, P. *J. Organomet. Chem.* **2001**, *625*, 195.
(15) Murugavel, R.; Davis, P.; Shete, V. S. *Inorg. Chem.* **2003**, *42*, 4696.
(16) Walawalkar, M. G. *Organometallics* **2003**, *22*, 879.
(17) Sathiyendiran, M.; Murugavel, R. *Inorg. Chem.* **2002**, *41*, 6404.
(18) Murugavel, R.; Sathiyendiran, M.; Walawalkar, M. G. *Inorg. Chem.* **2001**, *40*, 427.
(19) Murugavel, R.; Sathiyendiran, M. *Chem. Lett.* **2001**, 84.
(20) Anantharaman, G.; Walawalkar, M. G.; Murugavel, R.; Gábor, B.; Herbst-Irmer, R.; Baldus, M.; Angerstein, B.; Roesky, H. W. *Angew. Chem., Int. Ed.* **2003**, *42*, 4482.
(21) Yang, Y.; Pinkas, J.; Noltemeyer, M.; Schmidt, H.-G.; Roesky, H. W. *Angew. Chem., Int. Ed.* **1999**, *38*, 664.
(22) Mason, M. R.; Perkins, A. M.; Ponomarova, V. V.; Vij, A. *Organometallics* **2001**, *20*, 4833.
(23) (a) Azaïs, T.; Bonhomme, C.; Bonhomme-Coury, L.; Vaissermann, J.; Millot, Y.; Man, P. P.; Bertani, P.; Hirschinger, J.; Livage, J. *J. Chem. Soc., Dalton Trans.* **2002**, 609. (b) Azaïs, T.; Bonhomme-Coury, L.; Vaissermann, J.; Bertani, P.; Hirschinger, J.; Maquet, J.; Bonhomme, C. *Inorg. Chem.* **2002**, *41*, 981.
(24) Cassidy, J. E.; Jarvis, J. A. J.; Rothon, R. N. *J. Chem. Soc., Dalton Trans.* **1975**, 1497.
(25) Mason, M. R.; Matthews, R. M.; Perkins, A. M.; Ponomarova, V. V. *ACS Symp. Ser.* **2002**, *822*, 181.
(26) (a) Lafond, V.; Gervais, C.; Maquet, J.; Prochnow, D.; Babonneau, F.; Mutin, P. H. *Chem. Mater.* **2003**, *15*, in press. (b) Mehring, M.; Schürmann, S. *Chem. Commun.* **2001**, 2354. (c) Mehring, M.; Guerrero, G.; Dahan, F.; Mutin, P. H.; Vioux, A. *Inorg. Chem.* **2000**, *39*, 3325.
(27) Chandrasekhar, V.; Kingsley, S. *Angew. Chem., Int. Ed.* **2000**, *39*, 2320.
(28) (a) Lugmair, C. G.; Tilley, T. D.; Rheingold, A. L. *Chem. Mater.* **1997**, *9*, 339. (b) Lugmair, C. G.; Tilley, T. D. *Inorg. Chem.* **1998**, *37*, 1821. (c) Lugmair, C. G.; Tilley, T. D. *Inorg. Chem.* **1998**, *37*, 6304.

Scheme 3. Synthesis of New Copper−dtbp Complexes **1**−**3**

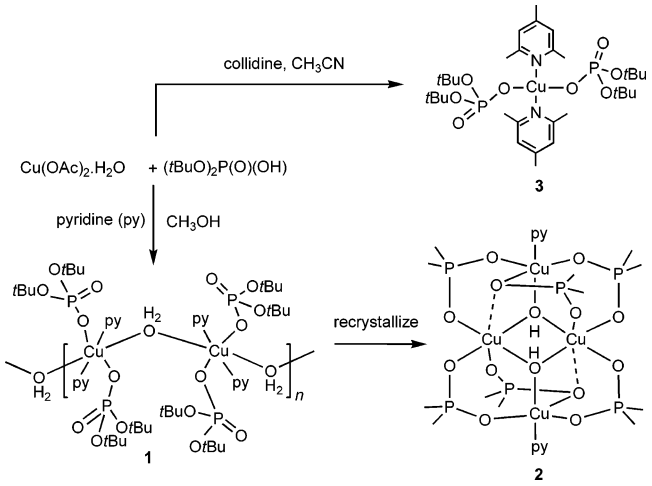

the crystals to be actually hollow tubes filled with mother liquor. Draining of the mother liquor from these tubes on a filter paper and subsequent air-drying produced pale-blue colored hollow tubes. Recrystallization of these tubes of **1** from the same solvent mixture gave, interestingly, a new green compound **2**. Preliminary chemical analysis revealed these compounds to be $[Cu(dtbp)_2(py)_2(OH_2)]$ (**1**) and $[Cu_4(\mu_3\text{-}OH)_2(dtbp)_6(py)_2]$ (**2**), respectively. Formation of **1** does not take place in the absence of pyrazine although it has not been possible to unravel the role played by it in the product formation. Similarly, the usage of coordinating solvents CH_3OH, THF, and DMSO is also essential although these solvent molecules do not get incorporated in the final product.[29]

Compounds **1** and **2** are air-stable, soluble in methanol, sparingly soluble in THF, and insoluble in hydrocarbons. The IR spectrum of **1** shows a broad absorption at 3170 cm^{-1} for the O−H stretching vibration. Strong absorptions at 1181, 1079, and 983 cm^{-1} indicate the presence of both symmetric and asymmetric POO vibrations in both **1** and **2**.[17,18,30] The UV−vis spectrum in methanol exhibits absorption maxima around 805 and 304 for **1** and 770 and 300 nm for **2**, respectively. While the absorption at 805 or 770 nm could be assigned to the d−d transitions of the copper ion, the absorption around 300 nm is due to the LMCT in the ultraviolet region.

To test the generality of the above reaction, the usage of 2,4,6-trimethylpyridine in place of pyridine was attempted. Thus, the reaction leading to **1** was repeated in CH_3CN with collidine as shown in Scheme 3.[31] Interestingly, this reaction proceeded smoothly to produce a deep-blue solution from which large dark-blue single crystals of **3** were obtained after a few days. Unlike **1**, the crystals of **3** were not hollow tubes but well-formed rectangular blocks. The elemental analysis for **3** revealed the compound to be $[Cu(dtbp)_2(collidine)_2]$, which is essentially same as the molecular formula for **1** but without one molecule of water. The IR spectrum of **3** is consistent with this observation, and no O−H absorption was observed around the characteristic region (3300−3500 cm^{-1}). The symmetric and asymmetric POO vibrations in the molecule result in absorptions at 1180, 1050, and 1010 cm^{-1}. The UV−vis spectrum of **3** showed an absorption in the visible region (796 nm) and a broad absorption in the ultraviolet region (302 nm), which were not useful in assigning any definite coordination geometry for the central copper atoms.

Although the analytical and spectroscopic studies provided the elemental composition, it was not possible to assign definitive structures of these molecules, especially given the ability of dtbp to act both as unidentate terminal and bidentate bridging ligand. Hence it was necessary to ascertain the molecular structures with the help of a single-crystal X-ray diffraction study in each case.

Molecular Structures. Since recrystallization of *blue* compound **1** invariably resulted in *green* compound **2**, the diffraction study of **1** was carried out by using a blue hollow tube obtained directly from the reaction.[32] A fairly flat rectangular portion of the hollow tube was obtained by scission under optical microscope and used for diffraction. The quality of the diffraction data obtained from this small plate was very poor and could not be improved by remeasuring the data with different platelets. The structure solution revealed that the asymmetric part of the unit cell of **1** contains two crystallographically independent half-copper atoms. Each of these independent copper atoms forms a one-dimensional zigzag polymer in the lattice, which contains a linear array of copper ions bridged by water molecules. Among the two crystallographically independent chains, one is well-behaved in terms of the final bond distances and angles, while the other chain suffers from severe disorder problems, especially in the positions of the phosphate groups. Hence, the discussion on the structure of **1** is fully based on the polymeric chain where no disorder problems have been encountered (Figure 1, Table 1).

The coordination environment of the copper atoms in polymer **1** could be termed as Jahn−Teller distorted octahedral arrangement (elongated along the *z*-axis). The equatorial positions around the copper atoms are occupied by two monodentate dtbp ligands (Cu(1)−O(1) 1.951(5) Å) and two pyridine molecules (Cu(1)−N(1) 2.000(7) Å). The individual Cu^{2+} ions in the polymeric chains are held together with the help of bridging water molecules which are present along the elongated Jahn−Teller axis (Cu(1)−O(5) 2.833(1) Å).[33,34] In the resultant polymer, the arrangement of the phosphate and pyridine ligands on adjacent copper atoms is staggered to overcome the steric repulsive forces (Figure 1). Due to the presence of a center of symmetry at copper and the fact

(29) The same reaction in the absence of these coordinating solvents (THF, DMSO, and DMF) yields the one-dimensional polymeric complex $[Cu(dtbp)_2]_n$, which has been reported by us recently,[17] and not the compounds **1** and **2**.

(30) (a) Thomas, L. C. *Interpretation of the Infrared Spectra of Organophosphorus Compounds*; Heyden and Son: Chichester, U.K., 1974. (b) Bellamy, L. J. *The Infrared Spectra of Complex Molecules*; Chapman and Hall: London, 1975.

(31) When this reaction was carried out in CH_3OH, as in the case of synthesis of **1**, only a greasy solid was obtained. Hence, it was necessary to change the solvent medium to acetonitrile.

(32) Several combinations of solvents tried to crystallize **1** either did not produce any single crystals or resulted in the formation of green compound **2**. Similarly, efforts to crystallize **2** from wet solvents did not produce the polymer **1**.

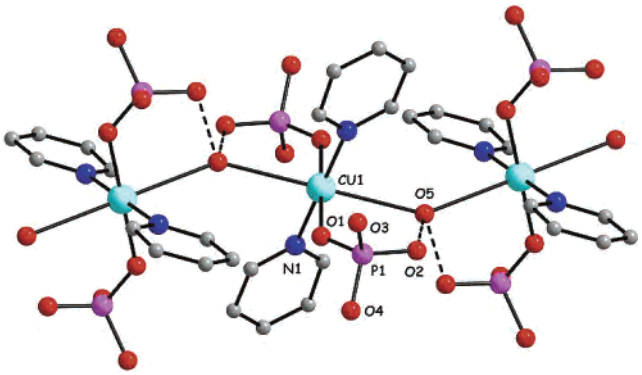

Figure 1. Section of the blue coordination polymer **1**. The hydrogen bonds between the water molecule and phosphoryl group are shown as broken bonds. The hydrogen atoms and the ^{t}Bu groups omitted for clarity.

Table 1. Selected Bond Lengths (Å) and Angles (deg) for Polymer **1**[a]

Cu(1)−O(1)	1.951(5)	P(1)−O(4)	1.577(6)
Cu(1)−O(5)	2.833(1)	P(1)−O(3)	1.580(6)
Cu(1)−N(1)	2.000(7)	N(1)−C(5)	1.330(11)
P(1)−O(1)	1.469(6)	N(1)−C(1)	1.330(12)
P(1)−O(2)	1.506(7)		
O(1)−Cu(1)−O(1)$^{\#1}$	180.0(2)	N(1)−Cu(1)−O(1)$^{\#1}$	88.1(3)
N(1)−Cu(1)−N(1)$^{\#1}$	180.0(4)	O(1)−Cu(1)−N(1)	91.9(3)
O(5)−Cu(1)−O(5)$^{\#1}$	180.0(2)	O(1)−Cu(1)−O(5)	89.4(2)
N(1)−Cu(1)−O(5)	89.0(2)	O(1)−Cu(1)−O(5)$^{\#1}$	90.6(3)
N(1)−Cu(1)−O(5)$^{\#1}$	91.0(2)		

[a] Symmetry transformations used to generate equivalent atoms: #1, $-x + 1/2, -y + 1/2, -z$.

that the dtbp, pyridine, and aqua ligands occupy trans positions, all trans angles around the metal are 180°. The cis angles in the molecule are close to the expected ideal value of 90° (88.1−91.9°).

Compound **2** crystallizes in the monoclinic space group *C*2/*c* with half of the molecule in the asymmetric part of the unit cell. The core structure of **2** is shown in Figure 2, and the selected bond distances and angles are listed in Table 2. The structure of **2** is a tetrameric copper cluster with a planar [$Cu_4(\mu_3$-OH)$_2$] core which is enveloped by dtbp ligands and pyridine molecules. Although there have been several examples of tetrameric copper clusters incorporating ligands such as alkoxides, siloxides, phosphinates, phosphonates, and carboxylates,[35−38] the inner Cu_4 unit in **2** is quite unique.

The four copper atoms in **2** are bridged by six dtbp ligands. There are two different types of copper centers. The two peripheral copper atoms (Cu(1) and Cu(1a)) have almost ideal tbp geometry. The triangular plane for these copper centers contains three bridging phosphate groups (O(2), O(6),

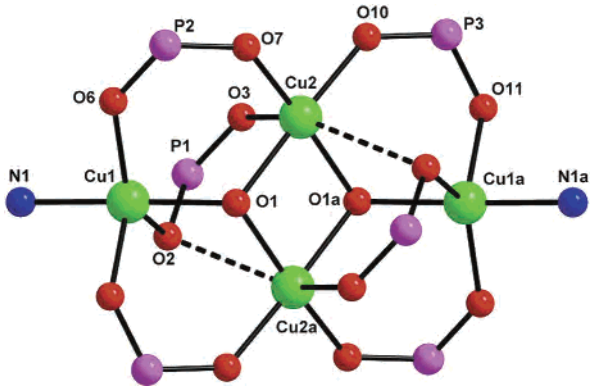

Figure 2. Inorganic core structure of the green tetramer **2**. The *tert*-butoxy groups, pyridine carbon atoms, and all hydrogen atoms are omitted for clarity.

Table 2. Selected Bond Lengths (Å) and Angles (deg) for the Tetrameric Complex **2**[a]

Cu(1)−O(6)	1.983(4)	P(1)−O(2)	1.506(4)
Cu(1)−O(1)	1.987(4)	P(1)−O(3)	1.509(5)
Cu(1)−N(1)	2.008(5)	P(1)−O(5)	1.592(5)
Cu(1)−O(11)$^{\#1}$	2.047(4)	P(2)−O(6)	1.480(5)
Cu(1)−O(2)	2.073(4)	P(2)−O(7)	1.494(4)
Cu(2)−O(7)	1.934(4)	P(2)−O(8)	1.564(5)
Cu(2)−O(10)	1.948(4)	P(2)−O(9)	1.579(5)
Cu(2)−O(1)$^{\#1}$	1.973(4)	P(3)−O(11)	1.483(4)
Cu(2)−O(1)	2.012(4)	P(3)−O(10)	1.498(4)
Cu(2)−O(3)	2.372(5)	P(3)−O(13)	1.572(5)
P(1)−O(4)	1.505(6)	P(3)−O(12)	1.579(5)
O(6)−Cu(1)−O(1)	91.6(2)	O(7)−Cu(2)−O(1)	90.9(2)
O(6)−Cu(1)−N(1)	90.5(2)	O(10)−Cu(2)−O(1)	177.5(2)
O(1)−Cu(1)−N(1)	177.0(2)	O(1)$^{\#1}$−Cu(2)−O(1)	81.0(2)
O(6)−Cu(1)−O(11)$^{\#1}$	119.4(2)	O(7)−Cu(2)−O(3)	107.6(2)
O(1)−Cu(1)−O(11)$^{\#1}$	89.6(2)	O(10)−Cu(2)−O(3)	88.7(2)
N(1)−Cu(1)−O(11)$^{\#1}$	91.2(2)	O(1)$^{\#1}$−Cu(2)−O(3)	82.0(2)
O(6)−Cu(1)−O(2)	133.2(2)	O(1)−Cu(2)−O(3)	92.1(2)
O(1)−Cu(1)−O(2)	84.9(2)	O(7)−Cu(2)−Cu(2)$^{\#1}$	130.4(1)
N(1)−Cu(1)−O(2)	92.1(2)	O(10)−Cu(2)−Cu(2)$^{\#1}$	137.7(1)
O(11)$^{\#1}$−Cu(1)−O(2)	107.2(2)	O(3)−Cu(2)−Cu(2)$^{\#1}$	86.2(1)
O(7)−Cu(2)−O(10)	91.0(2)	Cu(2)$^{\#1}$−O(1)−Cu(1)	113.1(2)
O(7)−Cu(2)−O(1)$^{\#1}$	167.8(2)	Cu(2)$^{\#1}$−O(1)−Cu(2)	99.0(2)
O(10)−Cu(2)−O(1)$^{\#1}$	96.8(2)	Cu(1)−O(1)−Cu(2)	116.9(2)

[a] Symmetry transformations used to generate equivalent atoms: #1, $-x + 1/2, -y + 1/2, -z + 1$.

O(11)) while the axial positions are occupied by a pyridine nitrogen (N(1)) and the μ_3-hydroxy group (O(1)). The two inner copper centers (Cu(2) and Cu(2a)) can be considered to have a square pyramidal or a pseudooctahedral geometry around them with five regular M−O bonds and one very weak M···O interaction. These metal centers are surrounded by two μ_3-hydroxy groups (O(1) and O(1a)) and two bridging

(33) The Jahn−Teller elongation of axial oxygen ligands results in Cu−O distances in the range 2.3−2.6 Å. In a recently synthesized copper phosphate, we have observed a Cu−O distance of 2.47 Å for the axial bonds.[19] In recent literature, other long Cu−O distances, ranging from 2.30 to 2.65 Å, have also been reported. The observed axial Cu−O bond in **1** is one of the longest reported in the literature (see ref 34).

(34) (a) Cano, J.; De Munno, G.; Sanz, J. L.; Ruiz, R.; Faus, J.; Lloret, F.; Julve, M.; Caneschi, A. *J. Chem. Soc., Dalton Trans.* **1997**, 1915. (b) Cotton, F. A.; Daniels, L. M.; Murillo, Quesada, J. F. *Inorg. Chem.* **1993**, *32*, 4861. (c) Simmons, C. J.; Hitchmann, M. A.; Stratemeier, H.; Schultz, A. J. *J. Am. Chem. Soc.* **1993**, *115*, 11304. (d) Hitchman, M. A.; Maaskant, W.; van der Plas, J.; Simmons, C. J.; Stratemeier, H. *J. Am. Chem. Soc.* **1999**, *121*, 1488. (e) Henning, R. W.; Schultz, A. J.; Hitchman, M. A.; Kelly, G.; Astley, T. *Inorg. Chem.* **2000**, *39*, 765.

(35) Tetrameric Copper Alkoxides: (a) Sirio, C.; Poncelet, Hubert-Pfalzgraf, L. G.; Daran, J. C.; Vaissermann, J. *Polyhedron* **1992**, *11*, 177. (b) Borup, B.; Huffman, J. C.; Caulton, K. G. *J. Organomet. Chem.* **1997**, *536/537*, 109. (c) Borup, B.; Folting, K.; Caulton, K. G. *Chem. Mater.* **1997**, *9*, 1021. (d) Brussaard, Y.; Olbrich, F.; Behrens, U. *J. Organomet. Chem.* **1996**, *519*, 115. (e) Purdy, A. P.; George, C. F. *Polyhedron* **1995**, *14*, 761. (f) Purdy, A. P.; George, C. F.; Brewer, G. A. *Inorg. Chem.* **1992**, *31*, 2633. (g) Neils, T. L.; Burlitch, J. M. *Inorg. Chem.* **1989**, *28*, 1607.

(36) Terameric copper siloxanes: (a) Molodtsova, Yu. A.; Pozdniakova, Yu. A.; Lyssenko, K. A.; Blagodatskikh, I. V.; Katsoulis, D. E.; Shchegolikhina, O. I. *J. Organomet. Chem.* **1998**, *571*, 31. (b) Edelmann, F. T.; Giessmann, S.; Fischer, A. *Inorg. Chem. Commun.* **2000**, *3*, 658.

(37) Chandrasekhar, V.; Kingsley, S.; Vij, A.; Lam, K. C.; Rheingold, A. L. *Inorg. Chem.* **2000**, *39*, 3238.

phosphate oxygen atoms (O(7) and O(10)) giving rise to a CuO_4 equatorial plane. The axial position is occupied by a bridging phosphate (Cu(2)−O(3) 2.372(5) Å). There is also an apparent sixth coordination site on the metal with a very weak M···O interaction (Cu(2)−O(2a) 2.875(5) Å). Interestingly, the intermetal distances in the cluster are short (Cu(2)−Cu(2a) 3.029(2), Cu(1)−Cu(2) 3.408(3), Cu(1)−Cu(2a) 3.304(2) Å) and, hence, interesting magnetic exchange properties are anticipated (vide infra).

After establishing the solid-state structures of both **1** and **2**, we further examined the structure of **1** to find any possible clues for the observed facile conversion of **1** → **2**. Interestingly, compound **1** has two short intrapolymer hydrogen bonds along the polymeric chain involving the coordinated water molecule and the two adjacent phosphoryl groups (O(2)···O(11) 2.65 Å; the dotted bonds in Figure 1) suggesting that this interaction may play a role in the conversion of water molecules to hydroxide anions, thus triggering the transformation of **1** to **2**. In fact, in one of the recently synthesized copper phosphates, it has been found that O−H···O═P bonds aid the lengthening of O−H bonds to result in longer D−H and shorter H−A distances.[9] If one were to consider a similar situation for **1**, it is reasonable to assume that the observed formation of **2** is partially facilitated by the presence of these very strong intrapolymer hydrogen bonds. However, it has not been possible to establish any conclusive experimental evidence for the participation of this hydrogen bonding in the conversion of **1** to **2** in solution. All the solution studies that have been carried out in the nonaqueous medium failed to give any clear indication for the conversion of μ-OH_2 ligand into a μ_3-OH ligand.

Hence, the formation of **2** should have essentially proceeded via the polymeric chain **1** falling apart in solution to monomeric species (a reasonable assumption considering very long Cu(1)−O(5) bond of 2.833(1) Å in **1**).[33,34] The tetrameric cage **2** can then assemble from these mononuclear species via the deprotonation of coordinated water molecules. This reorganization would have also been driven due to the fact that the formation of di-μ-hydroxo core is a thermodynamic sink in copper chemistry.[39,40]

Molecular Structure of 3. The absence of coordinated water molecule in **3**, as revealed by chemical analysis, has further been confirmed by a single-crystal X-ray diffraction study. The molecule of **3** crystallizes in the tetragonal space group $I4_1cd$. The structure of **3** is shown in Figure 3, and the selected bond distances and angles are listed in Table 3. The solid-state structure of **3** can be simply termed as the structure of **1** minus the bridging aqua ligands. As a result, the molecules of **3** are monomeric and the copper ions are tetracoordinate. The coordination geometry around the metal ion can be described as distorted square planar since the two set of angles observed in the molecular structure (85.5−95.4 and 160.1−174.8°) are closer to the expected ideal angles for square planar geometry. The two collidine molecules on the metal are trans to each other as the case with the two dtbp ligands. The observed Cu−O(P) distance in **3** (1.924(3) Å) is somewhat shorter than the average Cu−O(P) distances observed for **2**, where the dtbp ligands behave as bridging ligands 2.037(4) Å.

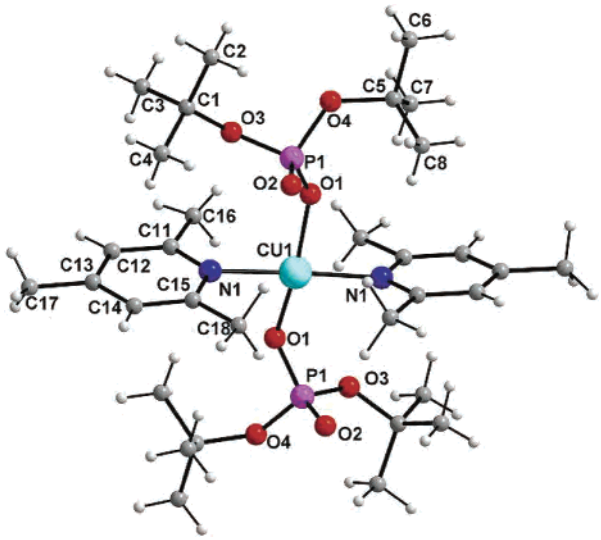

Figure 3. DIAMOND view of molecular structure of the monomeric complex **3**.

Table 3. Selected Bond Lengths (Å) and Angles (deg) for the Monomeric Phosphate **3**

Cu(1)−O(1)	1.924(3)	N(1)−C(11)	1.347(7)
Cu(1)−N(1)	2.046(3)	N(1)−C(15)	1.348(7)
P(1)−O(2)	1.470(4)	C(12)−H(12)	1.05(5)
P(1)−O(1)	1.518(3)	H(12)···O(4)$^{\#1}$	2.45(5)
P(1)−O(3)	1.592(3)	C(12)···O(4)$^{\#1}$	3.392(6)
P(1)−O(4)	1.601(3)		
O(1)−Cu(1)−N(1)	95.4(1)	O(2)−P(1)−O(3)	113.5(2)
O(1)$^{\#1}$−Cu(1)−N(1)	85.5(1)	O(1)−P(1)−O(3)	104.2(2)
O(1)$^{\#1}$−Cu(1)−N(1)$^{\#1}$	95.4(1)	O(2)−P(1)−O(4)	112.8(2)
O(1)−Cu(1)−N(1)$^{\#1}$	85.5(1)	O(1)−P(1)−O(4)	106.0(2)
O(1)$^{\#1}$−Cu(1)−O(1)	160.1(2)	O(3)−P(1)−O(4)	100.1(2)
N(1)−Cu(1)−N(1)$^{\#1}$	174.8(3)	P(1)−O(1)−Cu(1)	132.5(2)
O(2)−P(1)−O(1)	118.4(2)	C(12)−H(12)···O(4)$^{\#1}$	132.5(2)

[a] Symmetry transformations used to generate equivalent atoms: #1, $-x+1, -y, z$.

Although compound **3** does not form a polymeric structure with the help of bridging aqua ligands as in the case of **1**, the presence of intermolecular hydrogen bonding between the aromatic C−H groups of the collidine ring with phosphoryl oxygens of the dtbp from the adjacent molecule results in the formation of hydrogen-bonded one-dimensional polymeric network (Figure 4). The H(12) attached to C(12) forms an intermolecular hydrogen bond with phosphoryl O(4) of adjacent molecule as shown in Figure 4. The D···A bond distance and D−H···A angle involving this hydrogen bond (Table 3) are well within the range suggested for similar C−H···O hydrogen bonds.[41]

(38) Representative examples for other tetrameric copper complexes: (a) Little, R. G.; Moreland, J. A.; Yawney, D. B. W.; Doedens, R. J. *J. Am. Chem. Soc.* **1974**, *96*, 3834. (b) Oshio, H.; Saito, Y.; Ito, T. *Angew. Chem., Int. Ed. Engl.* **1997**, *36*, 2673. (c) Wegner, R.; Gottschaldt, M.; Görls, H.; Jäger, E.-G.; Kelmm, D. *Chem.—Eur. J.* **2001**, *7*, 2143. (d) Mukherjee, S.; Wehermüller, T.; Bother, E.; Wieghardt, K.; Chaudhuri, P. *Eur. J. Inorg. Chem.* **2003**, 863.

(39) For a review on compounds having stable $Cu_2(\mu\text{-}OH)_2$ core structure, see: Melnik, M. *Coord. Chem. Rev.* **1982**, *42*, 259.

(40) Also see: Sletten, J.; Sfrenson, A.; Julve, M.; Journaux, Y. *Inorg. Chem.* **1990**, *29*, 5054.

(41) Desiraju, G. R. *Acc. Chem. Res.* **1996**, *29*, 441.

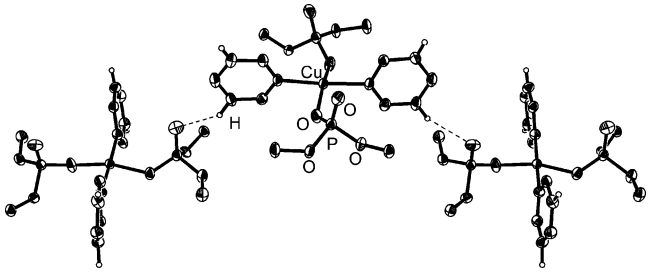

Figure 4. ORTEP of packing of **3**, showing the formation of 1-D polymeric chains through C−H···O hydrogen bonds between aryl C(12)−H(12) and P═O(4) groups of the adjacent molecules. All the methyl groups (both on collidine and dtbp) in the molecule are omitted for the sake of clarity.

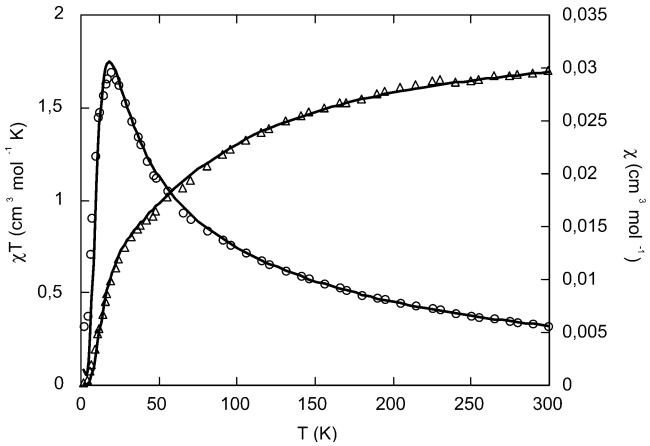

Figure 5. Plot of $\chi_M T$ vs T (denoted △) and χ_M vs T (denoted ○) for **2**. The solid lines represent the best fit in each case.

Magnetic Studies. The presence of multicopper assemblies in **1** and **2** warranted the investigation of their magnetic behavior. The magnetic studies of the complexes were performed on a SQUID magnetometer in the temperature range 300−2 K with an applied field of 3000 Oe. Since the structure of **1** shows that the bridging water molecules between the Cu^{2+} ions have a large separation (2.833(1) Å) due to tetragonal Jahn−Teller elongation, the magnetic orbital is well localized in the copper plane, thus leading to no magnetic interaction between the adjacent paramagnetic Cu^{2+} ions (see Supporting Information). However in the case of tetramer **2**, an interesting antiferromagnetic exchange interaction is observed (Figure 5). Considering the structure of the tetranuclear complex **2**, there are three different exchange-coupling parameters, viz. two different parameters between the peripheral Cu(1) and the two central Cu(2) and Cu(2a) (J_{p1} and J_{p2}) and one parameter between the two central Cu(2) atoms (J_c). However, since the Cu(1)−O(1)−Cu(2) and Cu(1)−O(1)−Cu(2a) angles are very close (106.7 and 113.3°, respectively), it is reasonable to assume that $J_{p1} = J_{p2} = J_p$. This leads to the following interaction topology:

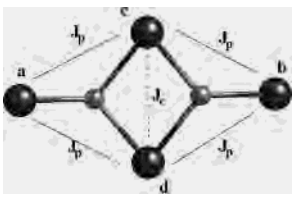

The spin Hamiltonian can thus be expressed as

$$H = -J_p(\mathbf{S_a} + \mathbf{S_b})\cdot(\mathbf{S_c} + \mathbf{S_d}) - J_c\mathbf{S_c}\cdot\mathbf{S_d}$$

where $\mathbf{S_a}$, $\mathbf{S_b}$, $\mathbf{S_c}$, and $\mathbf{S_d}$ are the local spin operators of the four Cu atoms. The vectorial model leads to the expression for the low-lying energy levels:

$$E(S,S_1,S_2) = -J_p[S(S+1) - S_1(S_1+1) - S_2(S_2+1)] - J_C[S_2(S_2+1)]$$

Here S_1 and S_2 are the intermediate spin values corresponding to $\mathbf{S_a} + \mathbf{S_b}$ and $\mathbf{S_c} + \mathbf{S_d}$, respectively, and S is the total spin. The $\chi_M T$ expression derived from the spin Hamiltonian is then

$$\chi_M T = (Ng^2\beta^2/k)[((2\exp(J_p/kT) + 2\exp(2J_p - J_c) + 2\exp(2J_p/kT) + 10\exp(3J_p/kT))(1-\rho))/(1 + 3\exp(J_p/kT) + 4\exp(2J_p - J_c) + 3\exp(2J_p/kT) + 5\exp(3J_p/kT)) + \rho]$$

assuming the same g value for all copper ions and ρ is the percentage of monomeric spin one-half impurities.

The fit of the experimental data for $\chi_M = f(T)$ and $\chi_M T = f(T)$ leads to $J_p = -42$ cm^{-1}, $J_c = -66$ cm^{-1}, $g = 2.25$, and $\rho = 0.8\%$ with an agreement factor $R = 10^{-4}$. Thus the ground state corresponds to the situation $S = 0$, $S_a + S_b = 1$, and $S_c + S_d = 1$. The first excited level is degenerate ($S = 0$, $S_a + S_b = 0$, $S_c + S_d = 0$ and $S = 1$, $S_a + S_b = 1$, $S_c + S_d = 0$) and is situated at $-4J_p + 2J_c$ above the ground state. The value of the exchange coupling parameter between the central Cu atoms ($J_c = -66$ cm^{-1}) is reasonable for a double hydroxo bridge with a Cu−O−Cu of 98.8°. The relatively weak J_p value between the peripheral and the central Cu atoms despite the rather large Cu−O−Cu angles can be understood by the presence of one hydroxo bridge instead of two between the central and the peripheral Cu atoms. This should roughly decrease the exchange parameter to the $^1/_4$ of its value since the exchange is proportional to the square of the energy difference between the magnetic orbitals.[42] Another effect that may contribute to the decrease of the exchange parameter is the presence of the phosphato ligand which has a countercomplementary effect to the oxo bridge as in the case of an acetate bridge.[43] However, this effect is probably not the dominant one because the delocalization of the d_{z^2}-type magnetic orbital toward the O(6) and O(11) is weak due to the tbp geometry of the peripheral Cu atoms.

Thermal Decomposition of 1−3. The presence of *tert*-butoxy groups makes compounds **1**−**3** ideal candidates for solid-state decomposition to produce phosphate materials. Moreover, the only coligand present in the complex, viz. pyridine in **1** and **2** (or collidine in **3**), is highly volatile and will not pose any problem during decomposition. To study the feasibility of using these compounds as precursors for the preparation of phosphate materials, their thermogravimer-

(42) Hay, P. J.; Thibeault, J. C.; Hoffmann, R. H. *J. Am. Chem. Soc.* **1975**, *97*, 4884.
(43) Nishida, Y.; Kida, S. *J. Chem. Soc., Dalton Trans.* **1986**, 2633. (b) McKee, V.; Zvagulis, M.; Reed, C. A. *Inorg. Chem.* **1985**, *24*, 2914.

Table 4. Summary of the TGA and Bulk Thermal Decomposition Studies for **1**−**3**

compd	primary decomp products	mater expected[a]	% wt loss[b] expt (theory)	secondary decomp product[c]	final mater[d]
1	pyridine, water, isobutene	$Cu(PO_3)_2$	66.1 (66.4)	P_2O_5	$Cu_2P_2O_7$ (major), $Cu(PO_3)_2$ (minor)
2	pyridine, water, isobutene	$2Cu(PO_3)_2 + Cu_2P_2O_7$	56.2 (56.3)	P_2O_5	$Cu_2P_2O_7$ (major), $Cu(PO_3)_2$ (minor)
3	collidine, water, isobutene	$Cu(PO_3)_2$	59.2 (59.4)	P_2O_5	$Cu_2P_2O_7$ (major), $Cu(PO_3)_2$ (minor)

[a] Based on Cu:P ratio in the respective precursor complex. [b] As per the TGA results; the calculated values are based on the material expected. [c] During bulk thermolysis on a tubular furnace at 500−510 °C for 2 days. [d] The bulk thermolysis product (characterized by PXRD, IR, and DR−UV).

tic analyses have been performed in an atmosphere of air.[44] The results obtained are listed in Table 4.

The TGA trace for **1** reveals the removal of coordinated water and pyridine molecules in the temperature range 50−100 °C. This is followed by the loss of isobutene from dtbp (140−160 °C) and the P−OH group condensation (>200 °C) to result in the formation of $Cu(PO_3)_2$ in the expected yield. The total weight loss of 66.1% observed at 400 °C corresponds to the loss of all volatiles (theoretical weight loss 66.4%) from **1** producing $Cu(PO_3)_2$. Similarly, the TGA for **2** reveals a major weight loss between 125 and 210 °C and a minor weight loss at 450 °C. The DTA trace shows the endothermic transition at 180 °C for the first weight loss where 12 isobutene and 2 pyridine molecules are lost. The second weight loss is due to the loss of water molecules. The total experimental weight loss of 56.2% agrees well with the complete removal of all volatiles at ∼400 °C (expected theoretical loss 56.3%). The percentage of the final material obtained from the initial precursor (43.8% of total weight of **2**) corresponds to the formation of $Cu_4P_6O_{19}$ (a mixture of $Cu(PO_3)_2$ and $Cu_2P_2O_7$).

The TGA of monomeric complex **3** reveals, as expected, three distinct weight losses in the temperature range 60−150, 160−195, and 200−350 °C corresponding to the loss of collidine, isobutene, and water molecules, respectively, to produce the copper metaphosphate material in 30.8% yield at 400 °C (expected 30.6%).

On the basis of the results obtained from TGA studies, bulk thermolyses of **1**−**3** were carried out in air in the temperature range 500−510 °C for 48 h. The final materials obtained from bulk thermolysis were characterized by PXRD[45,46] and IR and DR−UV spectroscopic techniques (see Experimental Section and Supporting Information). Irrespective of the starting molecular phosphate, the final material obtained in each case turned out to be predominately the pyrophosphate $Cu_2P_2O_7$ along with small amounts of the metaphosphate $Cu(PO_3)_2$. Even in the case of precursor complexes **1** and **3**, where the metal-to-phosphorus ratio is 1:2 (which is ideal for the formation of the metaphosphate $Cu(PO_3)_2$), the final material contains metal pyrophosphate as the major phase as revealed by PXRD studies.[45,46] The DR−UV results were also in agreement with the presence of both meta- and pyrophosphates in the final material.[47] While two separate absorptions were expected for the metaphosphate at around 825 and 1025 nm, a single absorption is expected for the pyroposphate at 925 nm in the visible region.[47] The products obtained by thermolyzing **1**−**3** show absorption due to both these forms.

Scheme 4. Suggested Decomposition Pattern of Copper−dtbp Complexes **1**−**3**

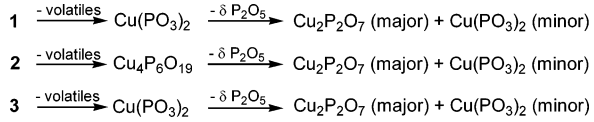

Contrary to the expected pure forms of phosphates from TGA studies (Table 4), the presence of both meta- and pyrophosphates was initially surprising. The well-documented relative thermal instability of the metalphosphate compared to the pyrophosphate, however, explains the observation.[48] It is known that when heated at high temperatures for prolonged periods, $Cu(PO_3)_2$ converts into $Cu_2P_2O_7$ by eliminating P_2O_5 ($2Cu(PO_3)_2 \rightarrow Cu_2P_2O_7 + P_2O_5$).[48] Thus, in the present study, when the samples were heated for 48 h at temperatures close to the boiling point of P_2O_5, further decomposition of the expected products (Table 4) takes place as per the equations shown in Scheme 4 to result in the mixture of the meta- and pyrophosphates.[49]

Conclusion

We have shown in this contribution that it is possible to generate a water-bridged copper phosphate polymer **1** and transform it to a novel tetramer **2** through a simple crystallization process. The molecular structure of **1** shows very strong hydrogen-bonding interactions involving the water hydrogen atoms and the uncoordinated phosphoryl group. Although it has not been possible to clearly establish a mechanism or a reaction pathway for the observed conversion of **1** into **2**, it appears that in solution the polymer breaks into monomeric form from which the tetramer is assembled through formation of a $[Cu_2(\mu_3\text{-}OH)_2]$ central core. The molecular structure of **3**, on the other hand, clearly reveals that both the increased hydrophobicity and the steric crowding due to the presence of three methyl groups on collidine are the reasons for copper ions rejecting additional aqua ligands in **3**. Hence, compound **3** stays as a monomeric square-planar complex while the copper ions in **1** become octahedral due to the extra room available for μ-OH_2 ligands. Thus, four different coordination geometries have been

(44) The TGA traces of compounds **1**−**3** are provided as Supporting Information.
(45) $Cu_2P_2O_7$: Powder Diffraction File, Card 44-0182, International Centre for Diffraction Data, Newtowne Square, PA, 1995.
(46) $Cu(PO_3)_2$: Powder Diffraction File, Card 29-0572, International Centre for Diffraction Data, Newtowne Square, PA, 1995.
(47) Ball, M. C. *J. Chem. Soc. A* **1968**, 1113.
(48) For a detailed discussion on the thermal stability of $Cu(PO_3)_2$, see: Bamberger, C. E.; Specht, E. D.; Anovitz, L. M. *J. Am. Ceram. Soc.* **1997**, *80*, 3133.
(49) It would be interesting to investigate the kinetics assoicated with the decomposition process by varying the temperature, time of thermolysis, and the rate of heating. Such a study is beyond the scope of this study and will be reported elsewhere.

observed for the copper ions in the three different copper−dtbp complexes reported in this paper.

Apart from the fact that both **1** and **2** represent new structural forms for copper complexes with any type of ligands, the presence of *tert*-butoxy groups make **1**−**3** good precursors for phosphate materials. Similarly we have shown that magnetic ordering takes place in the case of tetramer **2** at ∼20 K leading to antiferromagnetic coupling between the copper ions at this temperature. Our future studies in this area are aimed at unraveling the effect other types of auxiliary ligands in molecular copper phosphate chemistry.

Experimental Section

Instruments and Methods. All the starting materials and the products were found to be stable toward moisture and air, and no specific precautions were taken to rigorously exclude air. Elemental analyses were performed on a Carlo Erba (Milan, Italy) model 1106 elemental analyzer at IIT-Bombay. Infrared spectra were performed on a Nicolet Impact 400 or Nicolet AVTAR 320 spectrometer as KBr diluted disks. UV−visible spectral studies were carried out on a Shimadzu UV-260 spectrophotometer at room temperature. Powder XRD measurements were obtained on a Philips PW1729 X-ray powder diffractometer. The thermal analysis has been carried out in air with the heating rate of 10 °C min^{-1} on a DuPont thermal analyzer model 2100. The pH measurements were done on a Lab-India GMPH pH meter at ambient temperature.

Solvents and Starting Materials. Commercial grade solvents were purified by employing conventional procedures and were distilled prior to their use. Starting materials and commercial grade solvents were purified by employing conventional procedures and were distilled prior to their use. Commercially available starting materials such as $Cu(OAc)_2 \cdot H_2O$ (Fluka), pyridine (sd fine), pyrazine (Lancaster), and 2,4,6-trimethylpyridine (Lancaster) were used as received. Di-*tert*-butyl phosphate (dtbp-H) was synthesized from di-*tert*-butyl phosphite using a previously reported procedure.[50] Owing to its thermal instability, dtbp-H was freshly prepared from its potassium salt prior to its use.

Synthesis of $[Cu(dtbp)_2(py)_2(OH_2)]_n$ (1). Solid dtbp-H (420 mg, 2 mmol) and copper acetate monohydrate (200 mg, 1 mmol) were added to methanol (20 mL), and the resulting pale green solution was stirred for 15 min. Pyrazine (168 mg, 2 mmol) and THF (1 mL) were added to the above solution and stirred for 2 min. Subsequently pyridine (1 mL) and DMSO (5 mL) were added to the reaction mixture and filtered. The resultant blue solution (pH = 6.0) left at 25 °C for 48 h led to the formation of **1**. Yield: 482 mg (73%). Anal. Calcd for $C_{26}H_{48}CuN_2O_9P_2$ (M_r = 658.2): C, 47.5; H, 7.4; N, 4.3. Found: C, 46.3; H, 7.6; N, 5.0. IR (KBr, cm^{-1}): 3170 (w); 2973 (vs), 2934 (s), 1609 (s), 1478 (s), 1450 (s), 1390 (s), 1366 (vs), 1250 (s), 1182 (vs), 1062 (vs), 985 (vs), 913 (s), 827 (s), 756 (s), 709 (s), 645 (s), 594 (s). UV−vis (CH_3OH, nm): 805 (ϵ = 49 M^{-1} cm^{-1}), 304 (ϵ = 1244 M^{-1} cm^{-1}).

Synthesis of $[Cu_4(\mu_3\text{-}OH)_2(dtbp)_6(py)_2]$ (2). Compound **1** (143 mg, 0.22 mmol) was dissolved in a solvent mixture of methanol (10 mL), THF (1 mL), and DMSO (0.2 mL), and the resultant solution (pH = 5.4) was crystallized at 25 °C to obtain green crystals of **2** after 48 h. Yield: 55 mg (59%). Anal. Calcd for $C_{58}H_{120}Cu_4N_2O_{26}P_6$ (M_r = 1701.6): C, 40.9; H, 7.1; N, 1.7. Found: C, 39.2; H, 7.0; N, 1.7. IR (KBr, cm^{-1}): 2973 (vs), 2934 (s), 1482 (s), 1451 (s), 1392 (s), 1366 (vs), 1252 (s), 1209 (s), 1181 (vs), 1079 (vs), 983 (vs), 915 (s), 831 (s), 757 (s), 719 (s), 698 (s), 604 (s), 552 (s). UV−vis (CH_3OH, nm): 774 (ϵ = 164 M^{-1} cm^{-1}), 305 (ϵ = 5075 M^{-1} cm^{-1}).

Synthesis of $[Cu(dtbp)_2(collidine)_2]$ (3). Solid dtbp-H (420 mg, 2 mmol), copper acetate monohydrate (200 mg, 1 mmol), and 2,4,6-trimethylpyridine (1 mL) were added to acetonitrile (25 mL) in a beaker and heated on a water bath until all the solid copper acetate was dissolved. The resultant dark blue solution was filtered and left for crystallization. Large dark blue crystals of **3** formed from this solution after 3 days. Yield: 630 mg (88%). Anal. Calcd for $C_{32}H_{58}CuN_2O_8P_2$ (M_r = 724.28): C, 53.1; H, 8.1; N, 3.9. Found: C, 52.5; H, 7.9; N, 3.4. IR (KBr, cm^{-1}): 2980 (vs), 2950 (s), 1625 (s), 1595 (m), 1480 (s), 1340 (s), 1240 (s), 1220 (s), 1180 (s), 1050 (vs), 1010 (vs), 970 (vs), 950 (m), 850 (m), 680 (s), 600 (m), 510 (s). UV−vis (CH_3OH, nm): 796 (ϵ = 53 M^{-1} cm^{-1}), 302 (ϵ = 1845 M^{-1} cm^{-1}).

Thermal Decomposition of 1−3. Using the TGA data obtained on samples **1**−**3**, the thermal decomposition studies of the bulk samples were carried out on a temperature-controlled furnace. In a typical experiment, 2 g of the respective sample was placed on a alumina boat and heated in air at 500−510 °C for 48 h. The pyrolyzed samples were removed from the furnace, cooled to room temperature in a desiccator, and then used for the characterization experiments. The materials obtained were characterized by IR and DR−UV spectroscopic and PXRD studies. The traces of the TGA measurements, IR spectra, and PXRD profile of all the three pyrolyzed samples are given as Supporting Information. IR (KBr disk): for material obtained from **1**, 3400, 1170, 1085, 957, 726, 618, 582, 524 cm^{-1}; for material obtained from **2**, 3411, 1167, 1070, 959, 735, 617, 584, 524 cm^{-1}; for material obtained from **3**, 3412, 1167, 1074, 963, 735, 617, 590, 526 cm^{-1}. DR−UV: for material obtained from **1**, 300, 825, 925, 1025 nm; for material obtained from **2**, 300, 810, 920, 1020 nm; for material obtained from **3**, 305, 815, 925, 1020 nm.

X-ray Structure Determination of 1−3. The crystals for X-ray diffraction studies for compounds **1**−**3** were grown using the procedures described vide supra. A suitable single crystal of each compound was used for cell determination and intensity data collection either on a Nonius MACH 3 diffractometer (for **1** and **2**) at 293 K or a Siemens STOE AED2 diffractometer (for **3**) at 150 K. While the quality of the data obtained for **2** and **3** was found to be good, the poor quality of the crystal used for data collection resulted in very weak diffraction intensities for **1**. The structures of all three compounds were solved using direct methods as implemented in SHELXS-97,[51] and the structures were

(50) Zweirzak, A.; Kluba, M. *Tetrahedron* **1971**, *27*, 3163.

Table 5. Crystal Data and Structure Refinement Details for **1**−**3**

	1	**2**	**3**
empirical formula	$C_{26}H_{48}CuN_2O_9P_2$	$C_{58}H_{120}Cu_4N_2O_{26}P_6$	$C_{32}H_{58}CuN_2O_8P_2$
fw	658.14	1701.54	724.28
temp, K	293(2)	293(2)	203(2)
diffractometer	Nonius-MACH3	Nonius-MACH3	STOE-AED2
wavelength, Å	0.710 73	0.710 73	0.710 73
cryst system	orthorhombic	monoclinic	tetragonal
space group	Cccb	*C*2/*c*	$I4_1cd$
a, Å	26.808(6)	22.714(2)	19.961(3)
b, Å	45.570(6)	16.651(1)	
c, Å	10.818(2)	22.673(1)	19.041(4)
β, deg		94.14(6)	
V, Å^3	13796(6)	8563(1)	7587(2)
Z	16	4	8
d(calcd), Mg/m^3	1.267	1.320	1.268
abs coeff, mm^{-1}	0.772	1.159	0.707
F(000)	5584	3584	3096
cryst size, mm^3	0.1 × 0.1 × 0.1	0.4 × 0.35 × 0.25	0.9 × 0.8 × 0.6
θ range, deg	1.5−25.0	1.5−25.0	3.8−25.0
data/restraints/params	6050/49/361	7515/0/437	1760/1/255
goodness-of-fit on F^2	1.083	1.025	1.092
R1 [$I > 2\sigma(I)$]	0.1084	0.0602	0.044
R2 [$I > 2\sigma(I)$]	0.3080	0.1541	0.1123

refined using full-matrix least-squares method on F^2 using SHELXL-97.[52] In the case of **2** and **3** all non-hydrogen atoms were refined with anisotropic thermal parameters. The hydrogen atoms for **2** and **3** were fixed at calculated positions and were refined subsequently using a riding model. In the case of **1**, it was not possible to refine all non-hydrogen atoms with anisotropic thermal parameters and in the case of few atoms it was also necessary to use partial occupancies. The crystal data and selected details of the refinement are listed in Table 5. The details of final refined structures of all three compounds are provided as Supporting Information in the form of crystallographic information files (CIF).

The asymmetric unit in **1** contains the repeating unit of the two crystallographically independent polymeric chains. While one of the chains is structurally well-behaved, the other suffers from severe disorder problems, and hence, the structure could not be refined to completion. The discussion pertaining to this compound is mainly drawn from the polymeric chain without disorder problems.

Acknowledgment. This work was supported by the DST, New Delhi, through a Swarnajayanti Fellowship to R.M. We also thank the RSIC- and DST-funded single-crystal X-ray diffractometer facility at IIT-Bombay for characterization data. M.S. thanks the CSIR, New Delhi, for a Senior Research Fellowship. M.G.W. thanks the DST, New Delhi for the support in the form of a Fast Track Project.

Supporting Information Available: Details of X-ray structure determinations (as CIF files) and DR−UV, TGA−DTA, and magnetic susceptibility data (as PDF files). This material is available free of charge via the Internet at http://pubs.acs.org.

IC0349508

(51) Sheldrick, G. M. *SHELXS-97*: *Program for Crystal Structure Solution*; University of Göttingen: Göttingen, Germany, 1997.
(52) Sheldrick, G. M. *SHELXL-97: Program for Crystal Structure Refinement*; University of Göttingen: Göttingen, Germany, 1997.